Environmental Science
Processes & Impacts

Evaluating the pH-dependence of DOM absorbance, fluorescence, and photochemical production of singlet oxygen

Journal:	*Environmental Science: Processes & Impacts*
Manuscript ID	EM-ART-07-2023-000316.R1
Article Type:	Paper

The ionization state of dissolved organic matter impacts the role of DOM in natural and engineered systems, including DOM optical properties and photochemistry. This study links optical signals to structural moieties by investigating the pH dependence of absorbance, fluorescence, and photochemically produced singlet oxygen for diverse DOM samples.

Evaluating the pH-dependence of DOM absorbance, fluorescence, and photochemical production of singlet oxygen

Anya Allen,[1,2] Kai Cheng[2], Garrett McKay[2,]*

1. Department of Biochemistry and Biophysics, Texas A&M University, College Station, TX 77843
2. Zachry Department of Civil & Environmental Engineering, Texas A&M University, College Station, TX 77843

Corresponding author: 3136 TAMU, College Station, TX 77843; e-mail: gmckay@tamu.edu; phone: (979) 458-6540

Abstract

The protonation state of dissolved organic matter (DOM) impacts its structure and function in natural and engineered environmental systems, including DOM's ability to absorb light and form photochemically produced reactive intermediates (PPRI). However, the impacts of pH on DOM optical properties and PPRI formation have largely been evaluated separately, with less information being available on their interrelationship as a function of pH for the same set of samples. It is also unclear whether the impact of pH on optical spectra and associated optical surrogates for molecular size (e.g., E2:E3) of DOM isolates is representative of the behavior of whole water samples. To address these knowledge gaps, spectral pH titrations were performed for seven humic substance and natural organic matter isolates, three whole water samples, and three model compounds. Comparison of the fractional and differential absorption and fluorescence spectra between DOM isolates, whole water samples, and model compounds revealed similar spectral features between all samples. The results show that spectral features observed for DOM isolates also occur for whole water samples, which suggests that there is overlap in the types of chromophores present in DOM isolates and whole waters. Although results from model compounds overlapped with DOM, especially in the ultraviolet region of the spectrum, no model compound replicated DOM's pH dependence perfectly. By measuring apparent quantum yields of singlet oxygen (Φ_Δ), we show that aquatic DOM isolates exhibit a different pH-dependence ($\Phi_\Delta \propto pH^{-1}$) than soil-derived humic acid isolates ($\Phi_\Delta \propto pH$). For aquatic DOM isolates, Φ_Δ values measured at different pH were not correlated to apparent fluorescence quantum yields (Φ_f), suggesting that pH impacts singlet and triplet excited state DOM dynamics in different ways. In contrast, the proportional relationship

between Φ_f and Φ_Δ with increasing pH for soil humic acid isolates suggests that pH impacts singlet and triplet excited DOM in these samples in a similar fashion.

1 Introduction

The pH-dependent speciation of dissolved organic matter (DOM) has important implications for DOM reactivity in natural and engineered systems. For example, the impact of pH on the spectral shape and intensity of chromophoric dissolved organic matter (CDOM) and fluorescent dissolved organic matter (FDOM) could influence the interpretation of optical surrogates for DOM characterization and the formation of photochemically produced reactive intermediates (PPRI) from DOM photolysis. While the impacts of pH on DOM optical properties and PPRI formation have been studied previously,[1-6] they have largely been evaluated in separate studies on different samples. Less information is available about the interrelationship between optical properties and PPRI formation as a function of pH for the same set of samples, leading to several knowledge gaps, such as the lack of understanding of pH on DOM fluorescence quantum yields and whether such changes are coupled to PPRI quantum yields.

DOM is a heterogeneous assembly of organic molecules that collectively play essential roles in aquatic ecosystems.[7-9] The chemical composition and functionality of DOM is strongly influenced by source[10-12] and transformation pathways (e.g., photolysis and biotransformation).[13] On average, about half of the mass of DOM in aquatic environments can be classified as hydrophobic organic acids.[9] This fraction is abundant in aromatic carboxylic acids, (poly)phenols, and alkoxy phenols.[14, 15] Both carboxyl and phenol moieties speciate over environmentally relevant pH ranges (e.g., pH 5 to 9). Potentiometric titrations of DOM isolates indicate that the concentration of carboxyl and phenol moieties ranges from ~7.5 to 16 meq/g C and 0.7 to 2.6 meq/g C,[14, 15] respectively, and varies based on DOM source and isolation procedure. Generally, carboxyl contents are greater in terrestrial (i.e., soil-derived) fulvic acids, then, in decreasing order, aquatic fulvic acids, aquatic humic acids, and lastly terrestrial humic acids. Aquatic samples typically have a greater phenolic content than terrestrially derived samples.[14, 15]

Prior studies have shown that DOM absorbance spectra typically become shallower (lower spectral slope) and more intense (higher molar absorption coefficient) with increasing pH.[1, 6] This indicates that absorption in the visible region of the spectrum increases preferentially with increasing pH relative to absorption at UV wavelengths. Using differential absorption spectroscopy, Korshin and co-workers linked features in difference spectra ($\Delta A = A_{pH} - A_{pH,ref}$) to carboxyl and phenol moieties based on the pH-dependent changes in spectral features.[4] For example, at pH ~5 (near the pK_a of carboxylic acids), ΔA for aquatic fulvic acids shows a sharp peak at ~275 nm. Conversely, at pH ~9 (near the pK_a of phenols), ΔA shows a sharp peak at ~240 nm and a broad band with a maximum at ~375 nm. In addition to the recognized role of carboxylic and phenolic chromophores, spectral pH titrations of DOM isolates treated with sodium borohydride indicate that DOM chromophores also contain aldehyde and/or ketone moieties.[6]

Compared to absorbance, the impact of pH on FDOM spectral shape and intensity is more variable in the literature.[6, 16, 17] Studies using isolate materials have reported increasing fluorescence intensity as pH increases from acidic to neutral.[6] Other studies focused on whole water samples report conflicting results, with some indicating significant changes (typically an increase) in fluorescence emission with increasing pH[16] and others showing minor changes (< 10%).[17] These discrepancies show that it is still uncertain how pH impacts DOM fluorescence for whole water samples and whether isolate materials serve as a good proxy for these effects.

A related knowledge gap is the pH sensitivity of optical surrogates used for assessing DOM physicochemical properties like aromaticity and molecular weight. Although Groeneveld et al. showed that fluorescence-derived surrogates (e.g., fluorescence index (FI)) varied minimally between pH 5.5 and 7.5,[17] there is precedent suggesting that this may not be the case for all optical surrogates. For example, De Haan and De Boar showed that the E2:E3 ratio (i.e., absorbance at 250 nm divided by that at 365 nm) decreased from about 6 to 5 between pH 2 and 10.[2] It would be beneficial to know to what extent pH

impacts a broad set optical surrogates used for characterization of DOM isolates and whole waters. Finally, given the pH-dependence of DOM spectral shape and intensity, it is not surprising that PPRI quantum yields are also impacted by pH. Prior reports have shown that $^1O_2$ quantum yields (Φ_Δ) decrease with increasing pH.[3, 5, 18] $^1O_2$ is an important probe for triplet DOM (^{3}DOM*), an important oxidant in environmental photochemistry.[19] Thus, the pH-dependence of Φ_Δ may also serve as an indirect assessment of the pH-dependence of ^{3}DOM* quantum yields.

There are three primary objectives of this study: (1) To link DOM spectral signals to specific chromophores or groups of chromophores, (2) To evaluate the pH sensitivity of DOM optical surrogates, and (3) To assess the coupled pH-dependence of fluorescence quantum yields and $^1O_2$ quantum yields. To address these objectives, absorbance and fluorescence spectra were measured for seven humic substance and natural organic matter isolates, three model compounds (acetovanillone, 4-hydroxybenzoic acid, and autoxidized hydroquinone[20]), and three filtered whole water samples in one pH unit increments between pH 3 and 12. In addition, $^1O_2$ production under 365 nm irradiation was measured for DOM isolates between pH 4 and 9 in one unit increments. Φ_Δ were compared to apparent fluorescence quantum yields (Φ_f) to assess the extent to which pH impacts rates of non-radiative decay that may simultaneously influence fluorescence and $^1O_2$ production. While some studies have reported the impact of pH on optical properties and others have reported its effect on $^1O_2$ formation, our study performs both measurements on the same set of samples, exploring their collective significance.

2 Materials and Methods

2.1 Chemicals, DOM isolates, and sample preparation

DOM isolates were obtained from the International Humic Substance Society. Isolates include Suwannee River humic acid (SRHA, 3S101H), Suwannee River fulvic acid (SRFA, 3S101F), Suwannee River natural organic matter (SRNOM, 2R101N), Upper Mississippi River natural organic matter (MRNOM, 1R110N), Elliott Soil humic acid (ESHA, 5S102H), Pahokee Peat humic acid (PPHA, 1S103H), and Pahokee

Peat fulvic acid (PPFA, 2S103F). DOM stock solutions (~100 mg/L) were created by dissolving the solid isolate in lab grade water produced from a Barnstead Nanopure purification system (Thermo Scientific, 18.2 MΩ-cm resistivity). NaOH (0.1 M) was added incrementally until a pH ~7 was reached. After stirring for 24 h, stock solutions were filtered through pre-washed 0.45 μm syringe filters (polyethersulfone, VWR), and stored in amber bottles at 4°C in the dark. Details of the chemical reagents used in this study are listed in Table S1 of the Supporting Information.

Whole water samples were collected in muffled (500 °C, 4 h) amber glass bottles from the Brazos River (30.62687,-96.544133), Trinity River (32.740977, -97.354730), and Lake Bryan (30.712092, -96.457314). Samples were transported to the lab on ice and filtered using 0.45 μm polyether sulfone syringe filters within 24 h of collection.

To make solutions for titrations, DOM stocks were diluted in 10 mM, pH 7 phosphate buffer to 40 mg/L for SRFA, SRNOM, MRNOM, and 15 mg/L for SRHA, ESHA, PPHA, and PPFA. Concentrations were chosen to maximize fluorescence signal while maintaining a low enough optical density to allow for inner filter corrections. To prepare the autoxidized hydroquinone sample, 2 mM hydroquinone solution was prepared in 10 mM phosphate buffer at pH 7. This solution was allowed to sit at room temperature in an amber bottle for 1 month.[11] Stock solutions of 4-hydroxybenzoic acid and acetovanillone were diluted to 20 μM prior to pH titrations and optical measurements.

2.2 pH titrations

During titrations, pH was measured with a Thermo Scientific Orion VersaStar Pro pH meter and a combined pH microelectrode (Mettler-Toledo). Spectral pH titrations were initiated by decreasing the pH to 3 with 0.25 M HCl and then increasing pH in one-unit increments using 0.2 or 3 M NaOH. After each pH adjustment (pH tolerance of ± 0.1 within the target pH), absorbance and fluorescence spectra were measured using an Aqualog spectrofluorometer (Horiba Scientific) with a 1 cm quartz cuvette. The excitation wavelength was measured from 240 nm to 800 nm with 5 nm increments, with emission

wavelength being collected from 250 nm to 800 nm in ~2 nm increments. PPFA, MRNOM, SRNOM, and SRFA were measured with a 0.2 s integration time and ESHA, PPHA, and SRHA with a 0.5 s integration time. The process was repeated until measurements were collected from pH 3 to pH 12. Fluorescence spectra were corrected using the Aqualog software within the Sample Q procedure, which included blank subtraction, inner filter corrections, Rayleigh masking, and normalization to Raman scatter unit area at 350 nm excitation.[21] Lastly, baseline subtraction of absorbance spectra was performed by averaging absorbance signals between 750 and 800 nm and subtracting this average from the entire spectrum.

Optical spectra were not corrected for dilution caused by the addition of base for two reasons. First, the total volume change during titrations was 5% or less, which is smaller than the relative spectral intensities for samples one pH unit apart. Second, the pH titrations were performed with micropipettes, which sometimes necessitated adding drops of titrant (i.e., instead of dispensing the entire amount), making the estimation of total volume less precise. To address the impact of not correcting for dilution, pH titration of 10 mM phosphate was performed and the volume of titrant was recorded. The cumulative volumes added were used to calculate the dilution factors necessary to correct spectral data. Results from this analysis (Figure S1) show that while the absolute values for uncorrected spectra may differ from corrected spectra on the order of <5% between successive pH values, the pH-dependent trends are unaltered.

2.3 Optical metrics

Data analysis and plotting were performed in MATLAB (R2021a). To compare our results to past literature,[6, 22] a variety of metrics were calculated from the corrected absorbance and fluorescence spectra (Table 1).

Table 1. Quantitative metrics for evaluating optical changes during pH titration.

Optical metric	Equation	Description	Interpretation
Fractional absorbance	A_{pH_X}/A_{pH_3}	Absorbance at pH X divided by absorbance at pH 3	Larger A_{pH_X}/A_{pH_3} implies a greater relative absorbance gain with increasing pH

Mass-normalized differential absorbance	$\Delta A_{pH_X}/C$	Absorbance at pH X minus absorbance pH 3, normalized to concentration	Larger $\Delta A_{pH_X}/C$ implies a greater mass-normalized extinction gain with increasing pH
Fractional fluorescence[a]	F_{pH_X}/F_{pH_3}	Fluorescence at pH X divided by fluorescence at pH 3	Higher F_{pH_X}/F_{pH_3} implies a greater enhancement of fluorescence with increasing pH

[a]*F* refers to the fluorescence emission intensity at a single excitation wavelength (λ_{ex}) integrated over all emission wavelengths (λ_{em}), i.e., $F(\lambda_{ex}) = \int F(\lambda_{ex},\lambda_{em})d\lambda_{em}$.

Absorbance metrics included the fractional absorbance (A_{pH_X}/A_{pH_3}), which shows absorbance at pH X divided by absorbance of the sample at pH 3, and concentration-normalized differential absorbance ($\Delta A_{pH_X}/C$), which shows the absorbance at pH X minus absorbance of the sample at pH 3, all divided by the concentration (in mg/L) of sample. A higher A_{pH_X}/A_{pH_3}implies that absorbance is increasing with increasing pH and a more positive $\Delta A_{pH_X}/C$ implies a larger concentration-normalized extinction gain. The pH-dependence of fluorescence emission was evaluated using the fractional fluorescence change (F_{pH_X}/F_{pH_3}), which shows *F* at pH X divided by the *F* of the sample at pH 3. Here, *F* refers to the fluorescence emission intensity at a single excitation wavelength (λ_{ex}) integrated over all emission wavelengths (λ_{em}), i.e., $F(\lambda_{ex}) = \int F(\lambda_{ex},\lambda_{em})d\lambda_{em}$, which assesses all fluorophores excited at a particular wavelength. The λ_{ex} term is not shown in figure legends for simplicity. A higher F_{pH_X}/F_{pH_3} implies that fluorescence intensity is increasing with increasing pH. Optical surrogates based on absorbance (E2:E3, $S_{275\text{-}295}$, and S_R) and fluorescence spectra (FI, BIX) were calculated according to previously established methods.[23-25] Fluorescence quantum yields as a function of excitation wavelength were determined as described previously.[26]

2.4 Singlet oxygen measurements

Steady-state concentrations of $^1O_2$ ($[^1O_2]_{ss}$) were measured using furfuryl alcohol (FFA) as a probe compound.[27] Experiments were conducted with perinaphthenone (PN, 10 μM) or DOM (20 mg/L) as the sensitizer from pH 4 to 9 buffered by 10 mM phosphate. Solutions (25 mL) were prepared with 100 μM FFA and either DOM or PN and transferred to uncapped, borosilicate glass tubes for irradiation in a

Rayonett merry-go-round photoreactor equipped with mercury vapor lamps of emission maxima at 365 nm (see Figure S2). pH and absorbance at 365 nm showed minimal changes (<5%) between the beginning and end of each irradiation period. Small sample volumes (250 µL) were withdrawn periodically for analysis. Photochemical experiments at each pH were performed in triplicate. The concentration of FFA was monitored by ultra performance liquid chromatography (UPLC) coupled with diode array detector and C16 column (Ascentis Express 90 Å RP-Amide 15 cm × 4.6 mm, 5 µm, Supelco). The injection volume was 50 µL, and the thermostatic column compartment was set to 30 °C. The mobile phase was an isocratic mixture of 0.025 M ammonium acetate at pH 9.5 (A) and acetonitrile (B) with 75% A and 25% B. Total elution time was 3.5 min with a flow rate at 1 mL/min. FFA had a retention time of 1.9 min. The UV adsorption data at 219 nm were collected.

Photolysis experiments in the absence of sensitizer revealed no direct phototransformation of FFA. For experiments with DOM or PN as the $^1O_2$ sensitizer, the second-order rate constant between FFA and $^1O_2$ is well-characterized as 1.0×10^8 M^{-1} s^{-1} and used to calculate $[^1O_2]_{ss}$.[27] Singlet oxygen quantum yields for DOM (Φ_Δ) as a function of pH were calculated using the relative method, where perinapthenone ($\Phi_\Delta^{PN} = 1$) was used as the reference sensitizer, according to eq. 1

$$\Phi_\Delta = \frac{k_{obs}^{DOM} R_{abs}^{PN}}{k_{obs}^{PN} R_{abs}^{DOM}} \Phi_\Delta^{PN} \quad (1)$$

where k_{obs} represents the observed first order rate constant of FFA degradation and R_{abs} represents the rate of light absorption with respect to DOM or PN. Note that the photon irradiance ($I_{0,\lambda}$) and path length (ℓ) cancels because they are equivalent in the R_{abs} for both DOM and PN. Thus, the R_{abs} terms in eq. 1 were calculated by summing $1 - 10^{-A_\lambda}$ between 350 and 400 nm, where the A_λ term represents the total optical density of DOM ($\alpha_\lambda \ell$) or PN ($\varepsilon_{PN} c_{PN} \ell$) using the path length of 0.86 cm calculated based on the test tube geometry and diffraction.[28]

3 Results and Discussions

3.1 Impact of pH on absorbance and fluorescence of DOM isolates

For all DOM isolates, absorbance increased with increasing pH, but the magnitude of the changes depended on the excitation wavelength, pH range, and sample origin and isolation procedure (Figure 1). Taking SRFA as an exemplar (Figures 1A–C), absorbance increased with increasing pH (Figure 1A), with the greatest relative increases occurring in the visible light region (Figure 1B). The greatest gains in molar absorption coefficient occur beyond pH >7 and are associated with peaks centered at 300 nm and 375 nm (Figure 1C). Increases in $\Delta A/C$ are smaller at acidic to neutral pH (pH 3 to pH 7) than at basic pH (beyond pH 8). Another key observation for is that the differential absorbance spectral shape evolves as pH increases, with the peak at ~390 nm becoming the predominant feature at pH >7. This evolution of spectral features in $\Delta A/C$ plots is most noticeable for SRFA (Figure 1C) but also occurs for other aquatic isolates and PPFA (Figures 1G, 1K, 1O, and 1S). Such features are less prominent for soil humic acid isolates (Figures 1S and 1AA), which display mainly one feature centered ~290 nm.

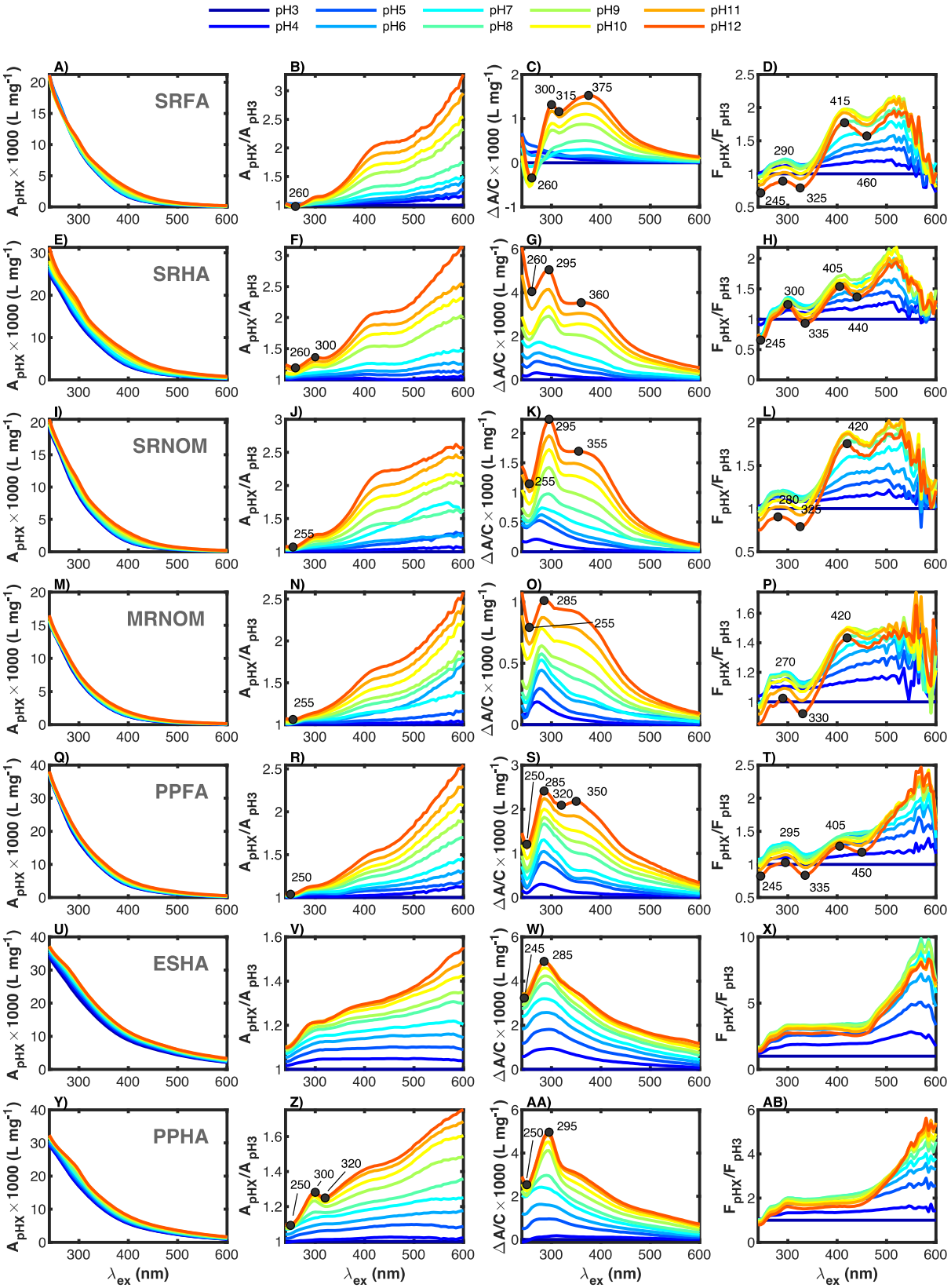
pH3
pH4
pH5
pH6
pH7
pH8
pH9
pH10
pH11
pH12
A)
SRFA
B)
C)
D)
E)
SRHA
F)
G)
H)
I)
SRNOM
J)
K)
L)
M)
MRNOM
N)
O)
P)
Q)
PPFA
R)
S)
T)
U)
ESHA
V)
W)
X)
Y)
PPHA
Z)
AA)
AB)
$A_{pHX} \times 1000$ (L mg^{-1})
A_{pHX}/A_{pH3}
$\Delta A/C \times 1000$ (L mg^{-1})
F_{pHX}/F_{pH3}
λ_{ex} (nm)

Figure 1: pH-Dependent spectra of A)-D) Suwannee River FA, E)-H) Suwannee River HA, I)-L) Suwannee River NOM, M)-P) Mississippi River NOM, Q)-T) Pahokee Peat FA, U)-X) Elliot Soil HA, and Y)-AA) Pahokee Peat HA. Spectra were collected during titrations initiated by acidifying solutions to pH 3 with 0.25 M HCl and then adding small amounts of 0.125 or 0.25 M NaOH to achieve one-unit pH increments. All spectra were measured in a 1 cm path length cuvette.

The pH dependence of absorption spectra shown in Figure 1 are consistent with those reported previously for DOM isolates from terrestrial and marine aquatic systems,[6, 29] soil isolates,[1] and biomass burning atmospheric brown carbon.[30] These pH-dependent absorption data have been interpreted in the context of the contribution of acidic functional groups in DOM, mainly phenols, which have pK_a values typically from 8 to 10, and carboxylic acids, which have pK_a values typically from 4 to 6. Phenols seem to be the major contributor given the more pronounced increases beyond pH 7 compared to more subtle gains between pH 3 and 7. The increase in absorbance with increasing pH likely arises from the increased electron-donating ability of phenolate ions (relative to phenol) and possibly the conformational changes in DOM molecules associated with this speciation.[6]

Fractional and differential absorbance spectra (Figure 1, columns 2 and 3) show features not observed in typical DOM absorption spectra (Figure 1, column 1). Many of these spectral features appear at similar wavelengths for all DOM isolates, suggesting a common structural origin. Similar to Schendorf et al.,[6] we observed that soil humic acids (ESHA and PPHA) exhibited the largest absorptivity gains (Figures 1W and 1AA), but the lowest fractional absorption increases (Figures 1V and Z). In contrast, PPFA and aquatic isolates exhibited greater fractional absorbance gains and lower absorptivity increases.

Fractional fluorescence (F_{pHX}/F_{pH3}) spectra provide a way to visualize how the total emission intensity at a given excitation wavelength changes with pH (Figure 1, column 4). Similar to $\Delta A/C$ spectra, F_{pHX}/F_{pH3} spectra show differing behavior over the pH ranges associated with deprotonation of carboxylic acids and phenols. At acidic pH, F_{pHX}/F_{pH3} spectra have fewer structural features. Prominent peaks at ~290 nm and ~410 nm appear at pH >7 for PPFA and aquatic isolates. In contrast, ESHA and PPHA have a different wavelength dependence, with F_{pHX}/F_{pH3} being wavelength-independent between an excitation

wavelength of ~300 to 450 nm. This wavelength-independence for ESHA and PPHA could imply that a structurally related group of fluorophores is being excited between 300 and 450 nm. Beyond ~475 nm, F_{pHX}/F_{pH_3} increases substantially for ESHA and PPHA, especially beyond pH 4.

An important observation for F_{pHX}/F_{pH_3} is that the fluorescence emission of DOM isolates has a maximum between pH 8 and 10 and then decreases with further increases in pH. This contrasts with a previous report suggesting that fluorescence emission was largely unchanged between pH 7 and 10.[6] For aquatic isolates and PPFA, fluorescence emission at pH 12 is the same or lower at pH 3 at excitation wavelengths less than ~350 nm, whereas emission in the visible region of the spectrum remains greater at pH 12. In contrast, ESHA and PPHA fluorescence emission at pH 12 remains higher than at pH 3 across the UV-visible spectrum.

Another observation from F_{pHX}/F_{pH_3} spectra is that, for aquatic isolates and PPFA, the increase in fluorescence emission with increasing pH is excitation wavelength-dependent (Figures 1D, 1H, 1L, 1P, and 1T), in contrast to a prior report that the emission gain was wavelength-independent.[6] These spectral features are consistent with the presence of unique fluorophores (or groups of fluorophores) in DOM (see Section 3.3).

3.2 Intercorrelation of absorbance and fluorescence changes

To gain further insight into the pH-dependent spectral changes, Figure 2 plots the fractional absorption (A_{pHX}/A_{pH_3}) versus the fractional fluorescence emission (F_{pHX}/F_{pH_3}) for DOM isolates as a function of excitation wavelength. Consistent with Figure 1, A_{pHX}/A_{pH_3} generally increases with increasing pH up to pH 12 regardless of excitation wavelength, whereas F_{pHX}/F_{pH_3} exhibits a maximum value around pH 8 to 10. PPFA and aquatic isolates can be visually differentiated based on the values of A_{pHX}/A_{pH_3} and F_{pHX}/F_{pH_3} and their proximity as a function of excitation wavelength. For example, for aquatic isolates and PPFA, A_{pHX}/A_{pH_3}– F_{pHX}/F_{pH_3} curves at λ_{ex}<300 nm are closely spaced, consistent with a structurally related group of chromophores and fluorophores being responsible for these signals. A_{pHX}/A_{pH_3}–F_{pHX}/F_{pH_3} curves

for ESHA and PPHA have different behavior, being more closely spaced between 300 and 450 nm, consistent with a single class of chromophores and fluorophores being excited in this wavelength region.

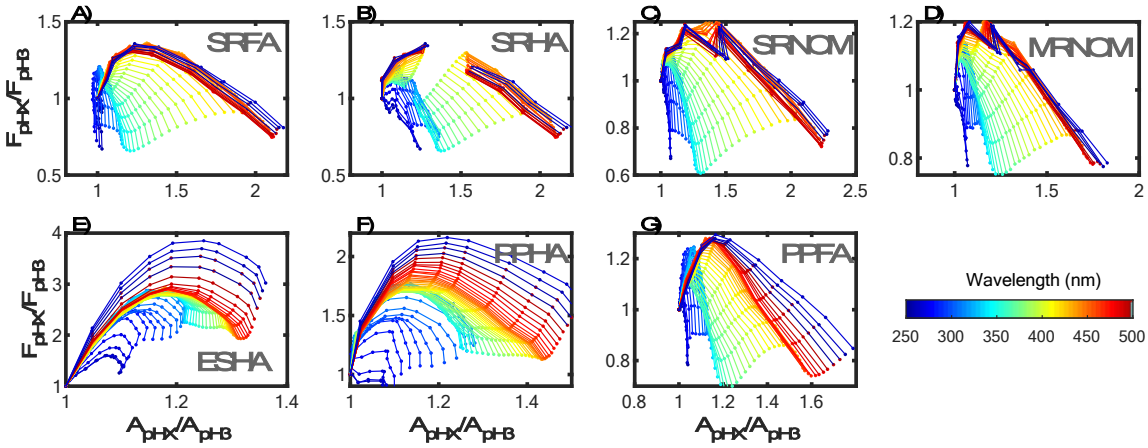

Figure 2: Change in integrated fluorescence vs. absorbance at pH 3 to 12 relative to pH 3 for aquatic and soil isolates. Markers represent a single pH and lines are linear interpolations between the markers. Colors shows increasing excitation wavelength (see legend). Values are missing for SRHA at pH 8.

The pH dependence of Φ_f is apparent from Figure 2. If the change in F_{pHX}/F_{pH3} between two pH values is greater than the change in A_{pHX}/A_{pH3}, this implies an increase in Φ_f between these two pH values. This is the case for ESHA and PPHA at most excitation wavelengths in the UV-visible. For aquatic isolates and PPFA, F_{pHX}/F_{pH3} is generally less than A_{pHX}/A_{pH3}, indicating that Φ_f generally decreases with decreasing pH. The excitation wavelength dependence of Φ_f and its dependence on pH is also shown in Figure S6.

3.3 Spectral pH titration of model compounds

pH-dependent absorbance and fluorescence spectra were measured for two model compounds (acetovanillone and 4-hydroxybenzoic acid) and autoxidized hydroquinone (Figure 3). Acetovanillone (AV) and 4-hydroxybenzoic acid (HBA) are not anticipated to form complexes in the ground or excited state and therefore are treated as non-interacting systems. In contrast, autoxidation of hydroquinone

and other aromatic compounds is known to produce complex chromophore systems that increase the possibility for inter- and intra-molecular interactions to contribute to optical signals.[20, 31]

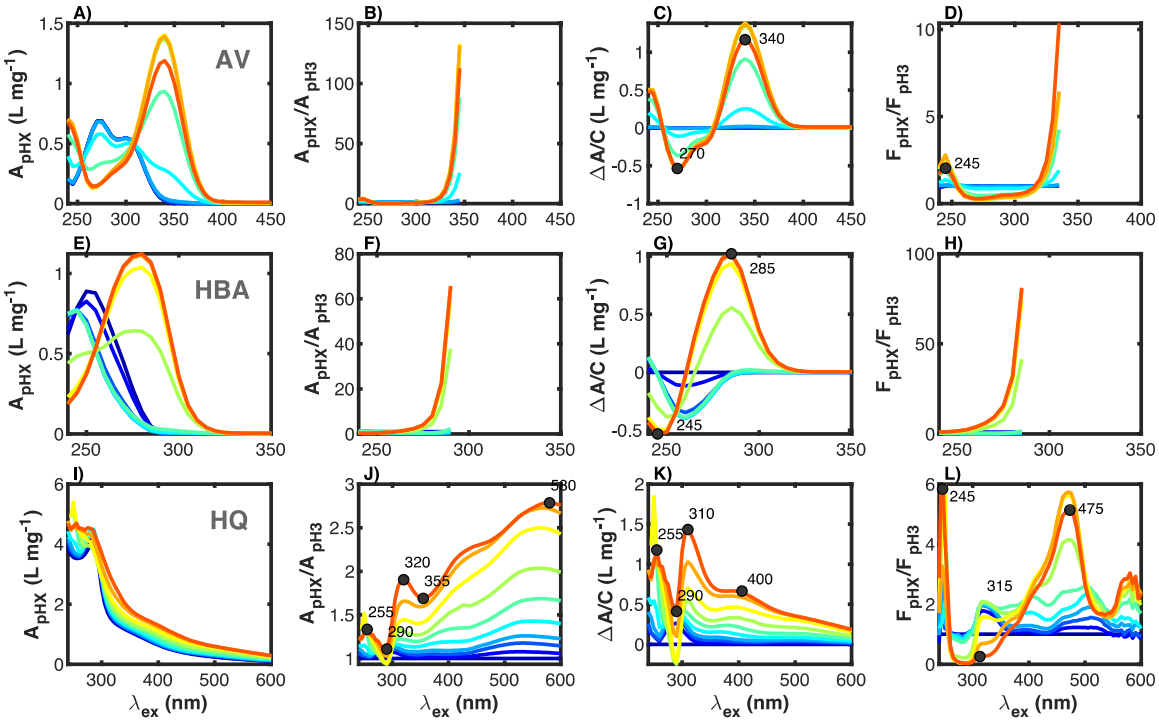

Figure 3: Mass normalized differential absorbance spectra ($\Delta A_{pH_X}/[DOM]$) and fluorescence spectra (F_{pH_X}) for A)–D) acetovanillone (AV), E)–H) 4-hydroxybenzoic acid (HBA), and I)–L) autoxidized hydroquinone (HQ) between pH 3 and 12. Titrations were performed by acidifying solutions to pH 3 with 0.25 M HCl and then adding small amounts of 0.125 or 0.25 M NaOH to achieve one-unit pH increments. Concentrations of each compound were: acetovanillone (20 µM, 3.32 mg/L), 4-hydroxybenzoic acid (20 µM, 2.76 mg/L), and autoxidized hydroquinone (initial hydroquinone concentration of 2 mM, 220 mg/L). Note that F_{pHX}/F_{pH3} in Figure 3 was not calculated if the absorbance at a given excitation wavelength was below ~0.01, which is five times the photometric stability of the Aqualog.

None of the fractional or differential spectra of the model systems (Figure 3) completely mimic the behavior of DOM, although there are some similarities. Of the model systems, autoxidized hydroquinone is most comparable to DOM samples, especially for absorption spectra. $\Delta A/C$ for autoxidized hydroquininone (Figure 3K) likewise increases with increasing pH, with a peak at ~310 nm and ~400 nm (the latter most evident at pH >8). Both peaks are slightly red-shifted relative to the peaks

observed for DOM isolates (~290 and ~375 nm, see Figure 1). The peak at ~285 nm for 4-hydroxybenzoic acid at pH >8 bears similarity to the peak at 285-295 in the differential absorption spectra for DOM samples (e.g., Figure 1O). The emergence of this feature at pH >8 for 4-hydroxybenzoic acid suggests that it is associated with deprotonation of the phenol moiety, not the carboxyl group.

Fractional fluorescence spectra of acetovanillone and 4-hydroxybenzoic acid increase with increasing excitation wavelength since red-shifted absorption bands appear with increasing pH. Note that F_{pHX}/F_{pH_3} in Figure 3 was not calculated if the absorbance at a given excitation wavelength was below ~0.01, which is five times the photometric stability of the Aqualog.[32] F_{pHX}/F_{pH_3} spectra for autoxidized hydroquinone did not resemble the typical behavior of DOM isolates (Figure 3L vs. Figure 1, column 1). F_{pHX}/F_{pH_3} for autoxidized hydroquinone had a prominent peak at ~475 nm beyond pH >8, which was absent for all DOM samples. Like DOM isolates, autoxidized hydroquinone exhibited a decrease in fluorescence emission between pH 11 and pH 12.

Results from the model compound studies provide evidence that 4-hydroxybenzoic acid could be responsible for the peak at ~290 nm in $\Delta A/C$ spectra of DOM. Likewise, the peak in $\Delta A/C$ spectra of acetovanillone (~340 nm) associated with deprotonation of the phenol moiety (pH > 8) could be partially responsible for the peak in differential absorption spectra of DOM at ~375 nm. While autoxidized hydroquinone and DOM exhibited some similarities in F_{pHX}/F_{pH_3} spectra, autoxidized hydroquinone had a strong peak 475 nm excitation wavelength, was especially responsive to pH >8 and absent for DOM isolates. This observation suggests differences in the structure of chromophores in DOM and autoxidized hydroquinone, despite their similar bulk optical characteristics and response to sodium borohydride reduction.[20] The nature and origin of these structural differences warrant further study.

3.4 pH titration of whole water DOM samples

To test whether the pH-dependent spectral changes observed for DOM isolates are representative of non-isolated materials, spectra were measured for three whole water samples titrated

between pH 3 and 12 (Figure 4). Two of the three samples (Brazos River and Lake Bryan) exhibited evidence of light scattering due to particulates at pH 12; thus, all pH 12 spectra were excluded from Figure 4 (see Figure S7 for pH 12 spectra). It is also important to note that absorption spectra during titrations were measured using a 10 cm path length cuvette (to increase the signal to noise ratio), but values in Figure 4 are normalized to a 1 cm path length.

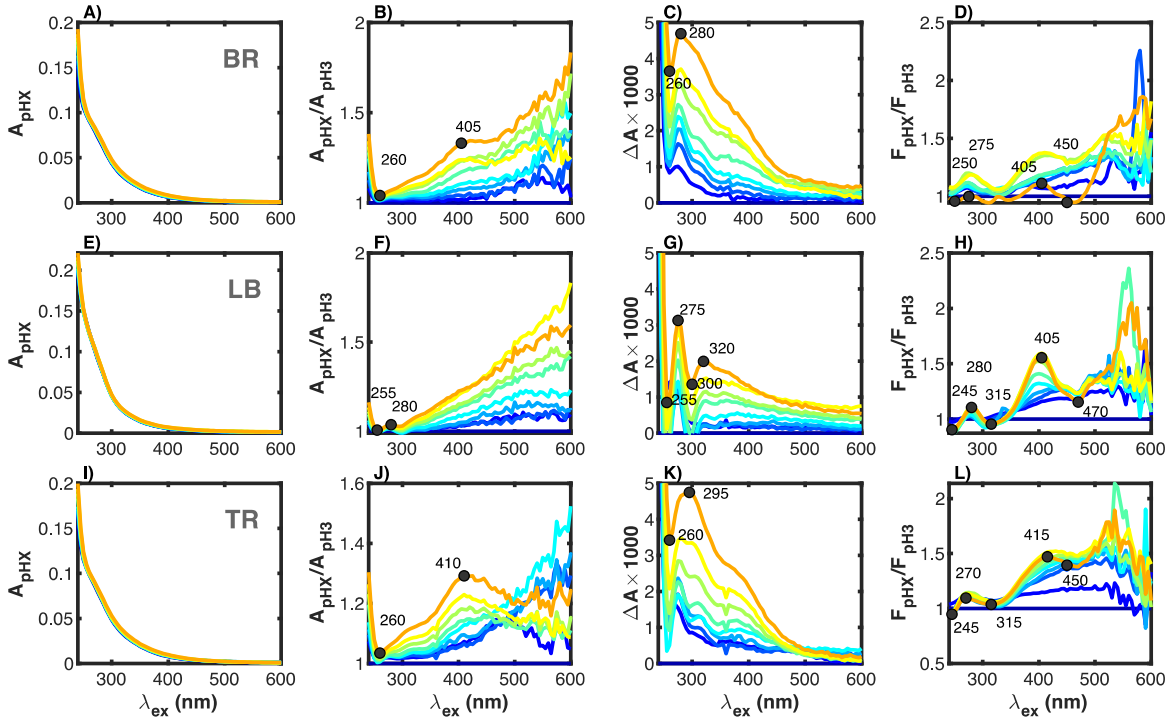

Figure 4: pH-Dependent optical properties of whole water samples from Central Texas, including A)-D) Brazos River (BR), E)-H) Lake Bryan (LB), and I)-L)Trinity River (TR). Spectra were collected during titrations initiated by acidifying solutions to pH 3 with 0.25 M HCl and then adding small amounts of 0.125 or 0.25 M NaOH to achieve one-unit pH increments. Spectra at pH 12 are excluded here due to particle formation and light scattering (see Figure SX). Absorbance spectra were collected in a 10 cm path length cuvette and normalized to a 1 cm path length. Linecolors correspond to legend in Figure 1.

Changes in the absorbance and fluorescence spectra of whole water samples during spectral pH titration were generally consistent with those of DOM isolates (e.g., A_{pHX}/A_{pH3} increased with increasing wavelength). Trinity River and Brazos River showed a peak in A_{pHX}/A_{pH3} spectra around 400 nm, especially at pH >9), consistent with DOM isolates. Differential absorption spectra likewise showed comparable features; a trough at ~260 nm, peak at ~270-290 nm, and, most noticeably for Brazos River and Trinity

River, a shoulder at ~390 nm. F_{pHX}/F_{pH3} spectra also show similarities between DOM isolates and whole water samples, with peaks at ~270 nm and ~400 nm. Fluorescence emission of whole water DOM decreases at pH 11 relative to pH 10 (Figures 4D, 4H, and 4L), consistent with the behavior of DOM isolates (see Figure 1).

The similarities in spectral features of DOM isolates and whole water samples suggests that DOM isolates can serve as a proxy for the pH-dependent behavior of whole water samples. The observation that F_{pHX}/F_{pH3} for whole water DOM decreased from pH 10 to 11 also matches the behavior of DOM isolates. One challenge for spectral pH titrations of whole waters is that the magnitude of the changes for whole water DOM was typically less than isolates (e.g., A_{pHX}/A_{pH3} <1.5). This lack of sensitivity may limit the ability to differentiate DOM source and structure between samples based on spectral pH titrations. Another challenge is the fact that water chemistry conditions (e.g., precipitation) may cause artifacts during spectral measurements such as light scattering. The impact of scattering can be addressed by visual inspection of the absorbance baseline at near IR wavelengths (a large baseline shift indicates scattering) as done in this study.

3.5 Impact of pH on optical surrogates

The impact of pH on absorbance- and fluorescence-based optical surrogates was evaluated by calculating E2:E3, $S_{275\text{-}295}$, S_R, FI, and BIX for DOM isolates and whole water samples between pH 3 and 12 (Figure 5 and SI Figure S8–S11). Of the DOM isolates, only results for SRFA, SRNOM, and MRNOM are displayed since these isolates are more representative of DOM in aquatic systems (e.g., compared to ESHA).

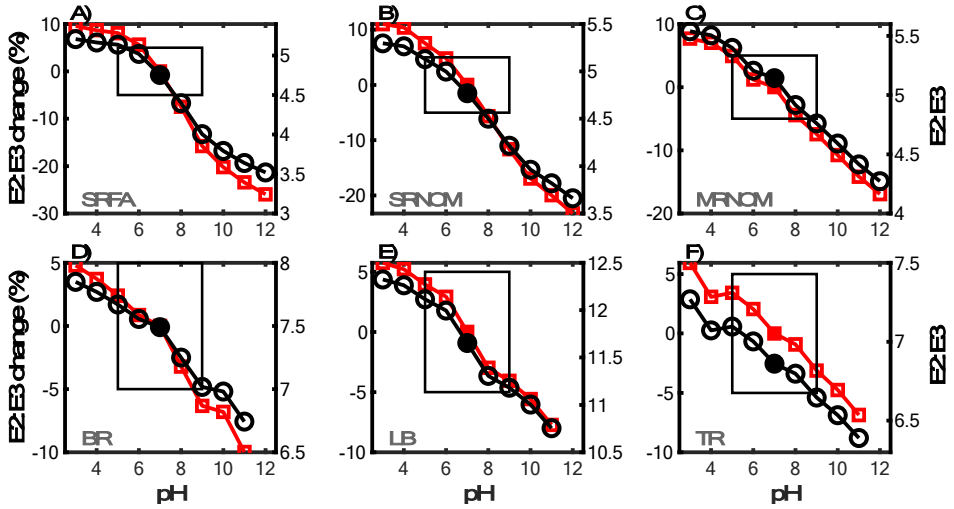

Figure 5: Variation in E2:E3 between pH 3 and 12 for DOM isolates and whole water samples. Gray box borders ± 5% relative change (red markers, left axis) and pH 5 to 9. The absolute change in E2:E3 is indicated by the black circles and right axis). pH 7 is indicated by the closed marker.

Consistent with De Haan and De Boar,[2] E2:E3 decreased with increasing pH, which is due to greater relative increases absorption at 365 nm. The percent difference from E2:E3 at pH 7 ranged from +10% (at pH 3) to –25 % (at pH 12). Within a narrower pH range of 5 to 9 (gray box in Figure 5), only DOM isolates had changes in E2:E3 greater than ± 5%. The three whole water sample's E2:E3 values remained within ± 5% between pH 5 and 9. $S_{275\text{-}295}$ was especially sensitive to pH beyond pH>7 for both DOM isolates and whole water samples (Figure S8). Consequently, S_R also showed a large pH dependence (Figure S9). Given the reproducibility of measurements of $S_{275\text{-}29,}$ and S_R (typically <5% coefficient of variance) and the observed dependence of these optical surrogate on pH, it is recommended that sample's pH be matched before measurement.

Compared to absorbance-based surrogates, pH had smaller impacts on FI and BIX such that not adjusting for pH within a narrow range (e.g., pH 6 to 8) should not impact interpretation of these surrogates. SRFA, SRNOM, and MRNOM all had minimal changes in FI between pH 6 to 8 (Figure S10), while at pH 9 SRFA and SRNOM FI values were more than 5% different than at pH 7. The FI of MRNOM was especially insensitive to pH. Two of the three whole water sample's FI values (Brazos River and Trinity

River) were insensitive to pH, whereas Lake Bryan exhibited more than an –5% decrease at pH 6 and more than a +5% increase at pH 9. Overall, these results are consistent with the conclusions of Groeneveld et al.[17] that impact of pH on FI and BIX is minimal between pH 5 to 9. Additional studies are needed to confirm this conclusion for whole water DOM samples from different geographic environments.

3.6 Impact of pH on quantum yields of photochemically produced $^1O_2$

In addition to the analysis on DOM optical properties, we evaluated the impact of pH on photochemically produced $^1O_2$. Φ_Δ values were measured between pH 4 and 9 using FFA and analyzed by relative sensitizer method.[33] The motivation for these experiments came from prior reports which have shown a simultaneous variation between Φ_Δ and Φ_{fi} for example, during ozonation.[34-36] We sought to determine if these correlations would remain consistent when observing changes in quantum yields under different pH conditions.

For aquatic DOM isolates and PPFA, Φ_Δ tended to decrease with increasing pH (Figures 6A and SI Figure S12). The difference in Φ_Δ between pH 4 and 9 ranged from ~60% reduction (for SRFA) to ~10% reduction (for PPFA). In addition, the pseudo-first-order rate constants (k_{obs}) of FFA remained relatively unaltered (or decreased slightly) between pH 4 and 9 for all aquatic DOM isolates and PPFA (Figure S13). R_{abs} also increased with increasing pH due to the greater absorption of DOM in the visible (Figure 1). Therefore, a roughly constant $[^1O_2]_{ss}$ and increased rate of light absorption with increasing pH gives rise to a decrease in Φ_Δ. The observed trend in decreasing Φ_Δ with increasing pH for aquatic DOM isolates is consistent with prior reports that have used similar irradiation wavelengths (e.g., UV-B). Frimmel et al. measured up to a 50% decrease in Φ_Δ between pH 3.5 and 10.5 with an aquatic fulvic acid extract.[3] Similarly, Dalrymple et al. found a similar pH dependence for SRNOM, for which Φ_Δ decreased 0.020 to 0.015 from pH 4 to 10.[18]

In contrast to aquatic isolates and PPFA, Φ_Δ values for soil humic acid isolates (ESHA and PPHA) increased with increasing pH, by up to 80% for ESHA. Both soil humic acid isolates exhibited an increase in k_{obs} with increasing pH, indicating an increase in $[^1O_2]_{ss}$. $[^1O_2]_{ss}$ measured in EHSA-sensitized solution increased by twofold from pH 4 to pH 9 (2.3 pM versus 4.6 pM) while the increase for PPHA was less (1.4 pM at pH 4 to 1.9 pM at pH 9). The increases in $[^1O_2]_{ss}$ with increasing pH outweighed the increases in R_{abs} for the samples. To our knowledge, there has been only one study that reported a positive correlation between Φ_Δ and pH, and this was for aquatic fulvic acid isolates using 532 nm laser excitation.[37]

Interestingly, the pattern in $^1O_2$ quantum yield observed from the DOM isolates is congruent with their optical characteristics (Figures 1 and 2). PPFA displayed optical behaviors more consistent with aquatic DOM, while ESHA and PPHA exhibited distinct characteristics typical of soil DOM. It is also worth noting that PPFA had the highest Φ_Δ values ($\approx$ 0.03) measured of all the DOM isolates (< 0.02).

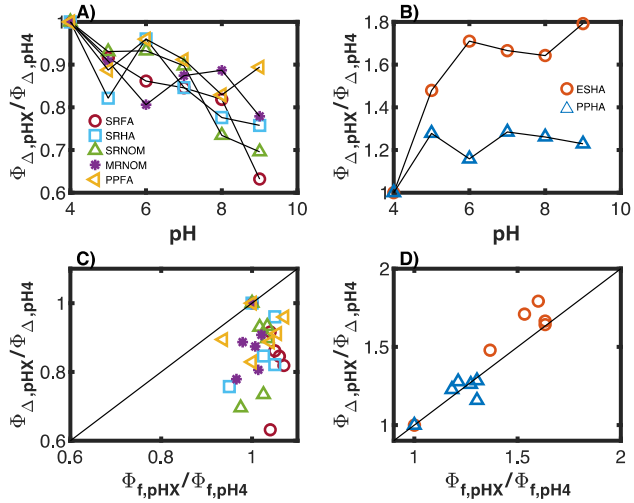

Figure 6: Relationship between singlet oxygen quantum yields ($\boldsymbol{\Phi_\Delta}$), pH, and fluorescence quantum yields ($\boldsymbol{\Phi_f}$). A and C) $\boldsymbol{\Phi_\Delta}$ from at pH 4 to 9 relative to $\boldsymbol{\Phi_\Delta}$ at pH4 versus pH. B) and D) Relative $\boldsymbol{\Phi_\Delta}$ versus relative $\boldsymbol{\Phi_f}$ over the same pH range. Legends in A) and B) correspond to C) and D), respectively. $\boldsymbol{\Phi_\Delta}$ determined using 100 µM FFA at pH 7 and 365 nm. $\boldsymbol{\Phi_f}$ corresponds to an excitation wavelength of 365 nm.

Relative changes in Φ_f with pH did not correlate to relative changes in Φ_Δ for aquatic isolates and PPFA (Figure 6C). This suggests that the overall small variation in Φ_f between pH 4 and 9 for these samples (less than ±10%) does not drive the larger changes (up to 40% decrease) in Φ_Δ. In contrast, the relative changes in Φ_f and Φ_Δ with varying pH for ESHA and PPHA generally followed a one-to-one relationship. One possible explanation is that, for PPHA and ESHA, fluorescence and singlet oxygen production arise from a structurally related set of chromophores.[34, 35] A second explanation is that ionization of carboxyl and phenol moieties causes a structural reorganization of DOM macromolecules. Increasing surface area to volume ratio with increasing repulsion of ionized moieties could decrease the extent of internal quenching of excited singlet DOM (^{1}DOM*) that are precursors to both fluorescence and triplet excited states (^{3}DOM*), the latter serving as a precursor to $^1O_2$.[38-40] Third, it should be noted that, as a hydrophilic probe, FFA quantifies aqueous phase $^1O_2$. Thus, the higher Φ_Δ for PPHA and ESHA at basic pH could be attributed to more $^1O_2$ reaching the bulk,[41, 42] aqueous phase due to a lesser extent of intra-DOM $^1O_2$ quenching for the more thread-like DOM structure at higher pH.[43] Finally, it is important to note that there has been some controversy about whether the conditions used extract humic substances from soil could cause structural modifications.[44, 45] It would be worth examining in future research whether soil-derived DOM obtained by aqueous extraction exhibits similar trends as the humic substance isolates studied here.

4 Conclusions

Spectral pH titrations of DOM isolates and whole water samples indicates that spectral features present in DOM isolate solutions are common to surface waters from Central Texas. These results suggest that the spectral response of DOM isolates during pH titration is a good proxy for what could be expected for whole water samples. Future studies should test this conclusion by pairing spectral pH titrations of whole water DOM and isolated materials.

Spectral pH titrations of three model compound systems provided insight into the origin of peaks in DOM differential absorption spectra, but none of the model systems matched DOM behavior across the entire UV-visible spectrum. Future research could expand on this approach by including more model compounds with different functional group combinations and by spectral pH titrations of mixtures of model compounds.[46]

One of the significant findings of this work is that most of the increases in DOM fluorescence emission occur in the pH range associated with deprotonation of carboxylic acids (pH 3 to 7) and that continued pH increases associated with deprotonation of phenols even lead to loss of emission intensity beyond pH >8. This loss in emission intensity occurs across the UV-visible spectrum, suggesting that it is associated with an increase in radiationless decay for ^{1}DOM* populations excited at all excitation wavelengths. This result is consistent with the overlap of emitting ^{1}DOM* species observed in our recent study on fluorescence quenching[47] and suggested previously by others.[40]

The impact of pH on the optical and photochemical properties of ESHA and PPHA (soil humic acid extracts) raises interesting points that challenge how optical properties are used for assessing DOM photochemistry. Increasing pH decreases these sample's E2:E3 values, which has classically been interpreted as a surrogate for increasing molecular size.[2, 48] Yet, Φ_Δ increased with increasing pH for these samples, whereas numerous prior studies have demonstrated positive correlations between Φ_Δ and E2:E3.[18, 49-52] This suggests that interpretation of Φ_Δ relationship to DOM optical surrogates (e.g., E2:E3) should be interpreted with caution in the absence of direct measurements of molecular size and chemical composition.

Results from this study indicate that $[^1O_2]_{ss}$ concentrations will be minimally impacted by pH in most aquatic systems, despite small decreases in Φ_Δ, due to the greater rate of light absorption at basic pH. Given that differences in Φ_Δ for aquatic isolates such as SRNOM and MRNOM are as great as 20%

between pH 4 and 9, we suggest that future studies evaluating the impact of chemical composition or optical properties on Φ_Δ of whole water samples harmonize the pH of all samples being studied.

5 Supporting Information

Supporting information is included free of charge on the RSC website.

6 Acknowledgments

The authors gratefully acknowledge support from the Army Research Office's Environmental Chemistry Program (W911NF-22-1-0086).

7 References

1. Baes, A. U.; Bloom, P. R., Fulvic Acid Ultraviolet-Visible Spectra: Influence of Solvent and pH. *Soil Science Society of America ...* **1990,** *54*, 1248-1254.
2. De Haan, H.; Werlemark, G.; De Boer, T., Effect of pH on molecular weight and size of fulvic acids in drainage water from peaty grassland in NW Netherlands. *Plant and Soil* **1983,** *75* (1), 63-73.
3. Frimmel, F. H.; Bauer, H.; Putzlen, J.; Murasecco, P.; Braun, A. M., Laser Flash Photolysis of Dissolved Aquatic Humic Material and the Sensitized Production of Singlet Oxygen. *Environmental Science & Technology* **1987,** *21* (6), 541-545.
4. Dryer, D. J.; Korshin, G. V.; Fabbricino, M., In Situ Examination of the Protonation Behavior of Fulvic Acids Using Differential Absorbance Spectroscopy. *Environmental Science & Technology* **2008,** *42* (17), 6644-6649.
5. Maizel, A. C.; Remucal, C. K., The effect of probe choice and solution conditions on the apparent photoreactivity of dissolved organic matter. *Environmental Science: Processes & Impacts* **2017,** *19* (8), 1040-1050.
6. Schendorf, T. M.; Del Vecchio, R.; Bianca, M.; Blough, N. V., Combined Effects of pH and Borohydride Reduction on Optical Properties of Humic Substances (HS): A Comparison of Optical Models. *Environmental Science & Technology* **2019,** *53* (11), 6310-6319.
7. Perdue, E. M.; Ritchie, J. D., *Dissolved organic matter in freshwaters*. Elsevier Amsterdam, Netherlands: 2003; Vol. 5, p 273-318.
8. Thurman, E. M., *Organic geochemistry of natural waters*. Kluwer: 1985.
9. Aiken, G. R.; McKnight, D. M.; Wershaw, R. L.; MacCarthy, P., *Humic Substances in Soil, Sediment, and Water: Geochemistry, Isolation, and Characterization*. John Wiley & Sons: 1985.
10. Weishaar, J. L.; Aiken, G. R.; Bergamaschi, B. A.; Fram, M. S.; Fujii, R.; Mopper, K., Evaluation of specific ultraviolet absorbance as an indicator of the chemical composition and reactivity of dissolved organic carbon. *Environmental Science & Technology* **2003,** *37* (20), 4702-4708.
11. McKnight, D. M.; Boyer, E. W.; Westerhoff, P. K.; Doran, P. T.; Kulbe, T.; Andersen, D. T., Spectrofluorometric characterization of dissolved organic matter for indication of precursor organic material and aromaticity. *Limnology and Oceanography* **2001,** *46* (1), 38-48.
12. Kellerman, A. M.; Guillemette, F.; Podgorski, D. C.; Aiken, G. R.; Butler, K. D.; Spencer, R. G. M., Unifying Concepts Linking Dissolved Organic Matter Composition to Persistence in Aquatic Ecosystems. *Environmental Science & Technology* **2018,** *52* (5), 2538-2548.
13. Cory, R. M.; Kling, G. W., Interactions between sunlight and microorganisms influence dissolved organic matter degradation along the aquatic continuum. *Limnology Oceanogr Lett* **2018,** *3* (3), 102-116.

14. Ritchie, J. D.; Perdue, E. M., Proton-binding study of standard and reference fulvic acids, humic acids, and natural organic matter. *Geochimica et Cosmochimica Acta* **2003,** *67* (1), 85-96.
15. Ritchie, J. D.; Perdue, E. M., Analytical constraints on acidic functional groups in humic substances. *Organic Geochemistry* **2008,** *39* (6), 783-799.
16. Spencer, R. G. M.; Bolton, L.; Baker, A., Freeze/thaw and pH effects on freshwater dissolved organic matter fluorescence and absorbance properties from a number of UK locations. *Water Research* **2007,** *41* (13), 2941-2950.
17. Groeneveld, M.; Catalán, N.; Einarsdottir, K.; Bravo, A. G.; Kothawala, D. N., The influence of pH on dissolved organic matter fluorescence in inland waters. *Analytical Methods* **2022,** *14* (13), 1351-1360.
18. Dalrymple, R. e. M.; Carfagno, A. K.; Sharpless, C. M., Correlations between Dissolved Organic Matter Optical Properties and Quantum Yields of Singlet Oxygen and Hydrogen Peroxide. *Environmental Science & Technology* **2010,** *44* (15), 5824-5829.
19. McNeill, K.; Canonica, S., Triplet state dissolved organic matter in aquatic photochemistry: reaction mechanisms, substrate scope, and photophysical properties. **2016,** *18* (11), 1381-1399.
20. McKay, G., Autoxidized Hydroquinone Mimics the Optical Properties of Chromophoric Dissolved Organic Matter. *Environ. Sci. Technol. Lett.* **2021,** *8* (9), 825-831.
21. Murphy, K. R.; Butler, K. D.; Spencer, R. G. M.; Stedmon, C. A.; Boehme, J. R.; Aiken, G. R., Measurement of Dissolved Organic Matter Fluorescence in Aquatic Environments: An Interlaboratory Comparison. *Environmental Science & Technology* **2010,** *44* (24), 9405-9412.
22. Li, H.; McKay, G., Relationships between the Physicochemical Properties of Dissolved Organic Matter and Its Reaction with Sodium Borohydride. *Environmental Science & Technology* **2021,** *55* (15), 10843-10851.
23. Helms, J. R.; Stubbins, A.; Ritchie, J. D.; Minor, E. C.; Kieber, D. J.; Mopper, K., Absorption spectral slopes and slope ratios as indicators of molecular weight, source, and photobleaching of chromophoric dissolved organic matter. *Limnology and Oceanography* **2008,** *53* (3), 955-969.
24. Cory, R. M.; Miller, M. P.; McKnight, D. M.; Guerard, J. J.; Miller, P. L., Effect of instrument-specific response on the analysis of fulvic acid fluorescence spectra. *Limnology and Oceanography: Methods* **2010,** *8* (2), 67-78.
25. Huguet, A.; Vacher, L.; Relexans, S.; Saubusse, S.; Froidefond, J. M.; Parlanti, E., Properties of fluorescent dissolved organic matter in the Gironde Estuary. *Organic Geochemistry* **2009,** *40* (6), 706-719.
26. McKay, G.; Korak, J. A.; Erickson, P. R.; Latch, D. E.; McNeill, K.; Rosario-Ortiz, F. L., The case against charge transfer interactions in dissolved organic matter photophysics. *Environmental Science & Technology* **2018,** *52* (2), 406-414.
27. Appiani, E.; Ossola, R.; Latch, D. E.; Erickson, P. R.; McNeill, K., Aqueous singlet oxygen reaction kinetics of furfuryl alcohol: effect of temperature, pH, and salt content. *Environmental Science: Processes & Impacts* **2017,** *19* (4), 507-516.
28. Wenk, J., The role of dissolved organic matter in aquatic photochemical oxidation processes. *Doctoral Dissertation* **2015,** 1-203.
29. Powers, L. C.; Vecchio, R. D.; Blough, N. V.; McDonald, N.; Schmitt-Kopplin, P.; Gonsior, M., Optical Properties and Photochemical Transformation of the Dissolved Organic Matter Released by Sargassum. *Frontiers in Marine Science* **2020,** *7*, 588287.
30. Phillips, S. M.; Bellcross, A. D.; Smith, G. D., Light Absorption by Brown Carbon in the Southeastern United States is pH-dependent. *Environmental Science & Technology* **2017,** *51* (12), 6782-6790.
31. Yakimov, B. P.; Rubekina, A. A.; Zherebker, A. Y.; Budylin, G. S.; Kompanets, V. O.; Chekalin, S. V.; Vainer, Y. G.; Hasan, A. A.; Nikolaev, E. N.; Fadeev, V. V.; Perminova, I. V.; Shirshin, E. A.,

Oxidation of Individual Aromatic Species Gives Rise to Humic-like Optical Properties. *Environ. Sci. Technol. Lett.* **2022**.

32. Scientific, H., Operation Manual. 2019; Vol. Revision K, p 340.

33. Ossola, R.; Jönsson, O. M.; Moor, K.; McNeill, K., Singlet Oxygen Quantum Yields in Environmental Waters. *Chemical Reviews* **2021**.

34. Leresche, F.; McKay, G.; Kurtz, T.; von Gunten, U.; Canonica, S.; Rosario-Ortiz, F. L., Effects of ozone on the photochemical and photophysical properties of dissolved organic matter. *Environmental Science & Technology* **2019,** *53* (10), 5622-5632.

35. Leresche, F.; Torres-Ruiz, J. A.; Kurtz, T.; von Gunten, U.; Rosario-Ortiz, F. L., Optical properties and photochemical production of hydroxyl radical and singlet oxygen after ozonation of dissolved organic matter. *Environmental Science: Water Research & Technology* **2021,** *7* (2), 346-356.

36. Buckley, S.; Leresche, F.; Hanson, B.; Rosario-Ortiz, F. L., Decoupling Optical Response and Photochemical Formation of Singlet Oxygen in Size Isolated Fractions of Ozonated Dissolved Organic Matter. *Environmental Science & Technology* **2023,** *57* (14), 5603-5610.

37. Pozdnyakov, I. P.; Salomatova, V. A.; Parkhats, M. V.; Dzhagarov, B. M.; Bazhin, N. M., Efficiency of singlet oxygen generation by fulvic acids and its influence on UV photodegradation of herbicide Amitrole in aqueous solutions. *Mendeleev Communications* **2017,** *27* (4), 399-401.

38. Sharpless, C. M., Lifetimes of Triplet Dissolved Natural Organic Matter (DOM) and the Effect of $NaBH_4$ Reduction on Singlet Oxygen Quantum Yields: Implications for DOM Photophysics. *Environmental Science & Technology* **2012,** *46* (8), 4466-4473.

39. Mostafa, S.; Rosario-Ortiz, F. L., Singlet oxygen formation from wastewater organic matter. *Environmental Science & Technology* **2013,** *47* (15), 8179-8186.

40. Sharpless, C. M.; Blough, N. V., The importance of charge-transfer interactions in determining chromophoric dissolved organic matter (CDOM) optical and photochemical properties. *Environmental Science: Processes & Impacts* **2014,** *16* (4), 654-671.

41. Latch, D. E.; McNeill, K., Microheterogeneity of singlet oxygen distributions in irradiated humic acid solutions. *Science* **2006,** *311* (5768), 1743-1747.

42. Cheng, K.; Zhang, L.; McKay, G., Evaluating the Microheterogeneous Distribution of Photochemically Generated Singlet Oxygen Using Furfuryl Amine. *Environmental Science & Technology* **2023,** *57* (19), 7568-7577.

43. Lan, T.; Wu, P.; Liu, Z. Y.; Stroet, M.; Liao, J. L.; Chai, Z. F.; Mark, A. E.; Liu, N.; Wang, D. Q., Understanding the Effect of pH on the Solubility and Aggregation Extent of Humic Acid in Solution by Combining Simulation and the Experiment. *Environmental Science & Technology* **2022,** *56* (2), 917-927.

44. Lehmann, J.; Kleber, M., The contentious nature of soil organic matter. *Nature* **2015,** *113* (7580), 143-9.

45. Kleber, M.; Lehmann, J., Humic Substances Extracted by Alkali Are Invalid Proxies for the Dynamics and Functions of Organic Matter in Terrestrial and Aquatic Ecosystems. *Journal of Environment Quality* **2019,** *48* (2), 207-10.

46. Zhang, C.; Mo, S.; Liu, Z.; Chen, B.; Korshin, G.; Hertkorn, N.; Ni, J.; Yan, M., Interpreting pH-Dependent Differential UV/VIS Absorbance Spectra to Characterize Carboxylic and Phenolic Chromophores in Natural Organic Matter. *Water Research* **2023,** *244*, 120522.

47. Li, H.; McKay, G., Fluorescence Quenching of Humic Substances and Natural Organic Matter by Nitroxide Free Radicals. *Environmental Science & Technology* **2023,** *57* (1), 719-729.

48. Peuravuori, J.; Pihlaja, K., Molecular size distribution and spectroscopic properties of aquatic humic substances. *Analytica Chimica Acta* **1997,** *337*, 133-149.

49. McKay, G.; Huang, W.; Romera-Castillo, C.; Crouch, J. E.; Rosario-Ortiz, F. L.; Jaffé, R., Predicting Reactive Intermediate Quantum Yields from Dissolved Organic Matter Photolysis Using

Optical Properties and Antioxidant Capacity. *Environmental Science & Technology* **2017,** *51* (10), 5404-5413.

50. Peterson, B. M.; McNally, A. M.; Cory, R. M.; Thoemke, J. D.; Cotner, J. B.; McNeill, K., Spatial and Temporal Distribution of Singlet Oxygen in Lake Superior. *Environmental Science & Technology* **2012,** *46* (13), 7222-7229.

51. Wan, D.; Wang, H.; Sharma, V. K.; Selvinsimpson, S.; Dai, H.; Luo, F.; Wang, C.; Chen, Y., Mechanistic Investigation of Enhanced Photoreactivity of Dissolved Organic Matter after Chlorination. *Environmental Science & Technology* **2021,** *55* (13), 8937-8946.

52. Berg, S. M.; Mooney, R. J.; McConville, M. B.; McIntyre, P. B.; Remucal, C. K., Seasonal and Spatial Variability of Dissolved Carbon Concentration and Composition in Lake Michigan Tributaries. *J Geophys Res Biogeosciences* **2021,** *126* (10), e2021JG006449.